International Journal of Engineering & Technology, 7 (4.30) (2018) 53-58

International Journal of Engineering & Technology

Website: www.sciencepubco.com/index.php/IJET

Research paper

Numerical Investigation on Effect of Rounded Cutting-Edge Radius and Machining Parameters in End Milling of AISI H13 Tool Steel

Husni Nazra Abu Bakar[1]*, Jaharah A. Ghani[2], Che Hassan Che Haron[3]

[1,2,3]Department of Mechanical and Material Engineering, Faculty of Engineering and Built Environment,
Universiti Kebangsaan Malaysia, 43600 Bangi, Malaysia
**Corresponding author E-mail:husninazra@gmail.com*

Abstract

Rounded cutting-edge radius is commonly applied to finish and semi-finish cutting, precision machining and micro-machining. The optimum effect is closely related to the work and tool material as well as machining parameters. However, for numerous cutting process, the optimal radius of rounded cutting-edge radius and machining parameters applied in the AISI H13 of end-milling is yet unknown Therefore, in improving tool life and cutting tool performance, a suitable design of cutting edge geometry regarding cutting edge-radius and machining parameters need to be examined and properly selected. In this regard, the paper deals to examine the effect of cutting edge-radius in rounded form and machining parameters of cutting force, cutting temperature and chip formation through the end-milling process of AISI H13 using uncoated cemented carbide cutting tool through finite element simulation of Thirdwave AdvantEdge 7.2 software. The machining parameters applied in the simulation setup were 200 and 240m/min of cutting speed, 0.03 and 0.06mm/tooth of feed-rate and axial depth of cut of 0.1 and 0.2mm while width of cut in radial direction was kept constant at 6.0mm. The cutting geometries includes the cutting-edge radius of 0.03 and 0.05mm and 10° of rake angle. The obtained results revealed that cutting forces and cutting temperature is increase as depth of cut in axial direction and cutting-edge radius increases while increasing value of speed and feed-rate of cutting resulted in decreasing cutting forces but increasing cutting temperature. The maximum cutting temperature is 674.91℃. The value obtained is lesser than the AISI H13 austenitizing temperature, therefore a layer known as white layer is supposedly hard to be created based on the cutting geometry and machining parameters applied.

Keywords: *Chip morphology; Cutting-edge radius; Cutting force; Cutting temperature; Thirdwave AdvantEdge.*

1. Introduction

Requirement for high productivity and reliability of machining process is noticeably urge in industry nowadays. One of the parameters that related to machining process in tooling is cutting edge radius. Few studies have conducted specifically on the cutting mechanisms of milling hardened steel (> 30 HRC) related to cutting edge radius and machining parameters using uncoated cemented carbide tool in observing the effect of cutting forces, cutting temperature and chip morphology. The suitable design of cutting edge radius and machining parameters hence can significantly affect the performance of a tool and stability of machining process in terms of material deformation and flow, tool wear and cutting forces as well as heat distribution, tool-chip friction, roughness of machined surface and residual stresses [1,2].
Three fundamental cutting-edge shapes which are rounded, sharp and chamfered are defined as shown in Fig. 1[3,4]. Regarding the rounded edge, the geometry can be either in single radius, trumpet form or waterfall form and it is based on the contour of tool face A_γ and tool flank A_α that is connecting to each other. A nominal single cutting-edge radius r_n is considered if the transition amid them is uniformly created without strong variations along the rounded profile. On the other hand, the geometry of the trumpet and waterfall form is considered when the rounded contour is highly arc in shape along the rounded profile. The joint points of the rounding profile depending on the rounding lengths of S_α and S_γ. Rounded edges are classified if cutting-edge radius r_n is between range 5 and 50 µm, whereas cutting edge radius whose radius r_n less than 5 µm is classified as sharp edges [4]. The intersection of tool face A_γ and tool flank A_α defines sharp edges. In actual, cutting edge which is sharp in edge is impossible to be produced because of its lower stability against mechanical loads, thus is not suitable for many machining tasks [4-6]. Chamfered edge is generated through the joining of the flat surface either chamfer or land of tool face A_γ also tool flank A_α. Chamfer length b_n, land length b_y as well as chamfer angle y_b can give an effect to the flat surface characteristics.
Wang et al. [7] studied the consequences of milling 30Cr3SiNiMoVA Steel using rounded cutting-edge radius on cutting forces and cutting temperature using finite element simulation. According to the authors, increasing the cutting-edge radius give rise to cutting forces as well as cutting temperature. The results of cutting forces is also supported by Afazov et al. [8] which stated cutting forces increase as cutting-edge radius increases. Results of cutting temperature is also supported by M.Saoubi et al. [9] and Outerio et al. [10] which reveal that increasing cutting edge radius as of 2 to 25µm then 44 to 55µm respectively resulted in rising of cutting temperature. Zhang et al. [11] and Riza et al. [12] studied effect of machining parameters on milling AISI H13 steel towards cutting forces and temperature using finite element simulation and experimental analysis respectively.

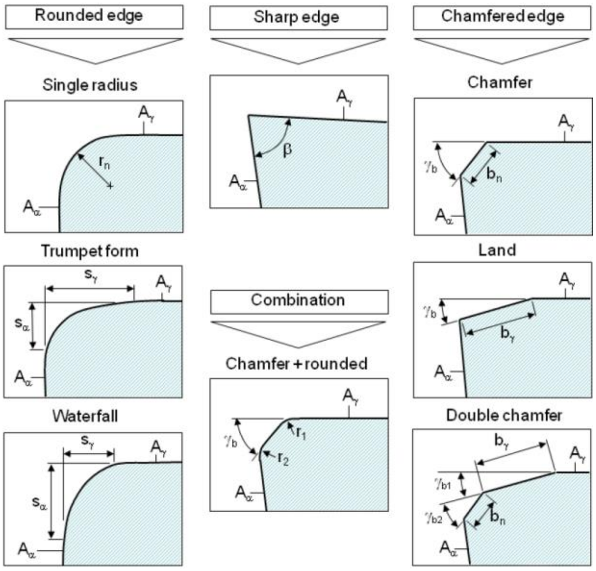

Fig. 1: Variations of cutting-edge shapes

The results of both investigations show that rising of feed-rate and cutting speed value lead to increase of forces and temperature in the cutting process, respectively. Several types in thermal damage, both for cutting tool and workpiece, such as rapid tool wear is determined because of high temperature generated during machining process [13,14]. Wang et al. [15] evaluated through simulation process the outcome of material hardness and speed of the cutting towards cutting forces and chip morphology on AISI D2 hardened tool steel. Results of the evaluation show that cutting forces give vigorous and important effect and serrated chips are produced as the cutting speed and workpiece hardness increases. Cui et al. [16] investigated the research on AISI H13 high speed face milling (46-47 HRC) to find the features of tool wear, cutting forces and formation of chip through various value of cutting speed. The author observed that cutting forces and chip segmentation rises when the value of the cutting speed increases but is opposite trend in tool life. Furthermore, research done on longitudinal type of turning process using cutting tool of coated cemented carbide by Outeiro [17] on AISI H13 steel (51HRC) revealed that, the most significantly parameters affected for maximum residual stresses are cutting-edge radius and feed-rate where reducing feed-rate and increasing cutting-edge radius lead to decreases in magnitude of tensile residual stresses. Li et al. [18] was done the study on AISI H13 steel (50±1 HRC) dry hard milling and perform the outcome of characterization of chip microstructure using hone type cutting-edge radius. The results revealed that, larger hone type cutting-edge radius generates white layer which is thicker at the back surface of chip, induces greater temperature and producing saw type of tooth chips.

The aim of this paper is to explore effect of cutting-edge radius and machining parameters towards various machining performance such as cutting forces, cutting temperature and formation of chip through the process of end milling AISI H13 steel using uncoated cemented carbide cutting tool by finite element simulation of Thirdwave AdvantEdge software.

Hot work AISI H13 tool steel is characterized as having an excellent in mechanical properties, for instance, it has high thermal softening, hardenability, strength and toughness. Thus, it is usually applied in industrial background, where the applications used for hot working process of hardness criteria ranging from 44 to 48 HRC while forging process and extrusion dies process ranging between 46 to 49 HRC. Furthermore, process of tools blanking and tools bending applied hardness between 50 to 52 HRC while swaging dies took the hardness of 53 to 55 HRC. On the other hand, die casting applied the hardness between 52 to 54 HRC also injection molding and further applications for the macro and micro-scale size [19,20].

2. Methodology

2.1. Finite element simulation setup

AISI H13 tool steel was simulated through oblique cutting process using a commercial finite element software, with a Lagrangian, explicit and dynamic code, Thirdwave AdvantEdge version 7.2. Thirdwave AdvantEdge is one of the software which commercially developed to simulate machining with the aiming is to assist customers in machining process as regards on designing, improving as well as optimising the processes. To get finite element results in more detailed, meshing of workpiece through the highest nodes of 24 000 was applied and 0.1mm maximum size of element and 0.2mm minimum size of element was selected. Meanwhile, 2 and 6 as the default value was set as factor for mesh refinement and coarsening, respectively. Cutting process was performed using 6 mm diameter, 4 flutes of uncoated end mill type of cutting tool while cemented carbide of K Grade was applied as it tool material. The material of the workpiece was AISI H13 with the hardness of 52 HRC. The parameters used in the simulation was tabulated in Table 1 whereas Table 2 tabulated chemical composition for the wokpiece material.

Table 1: Parameters applied in finite element simulation of AdvantEdge

Parameters	Values
Cutting speed (m/min)	200, 240
Feed-rate (mm/tooth)	0.03, 0.06
Axial depth of cut (mm)	0.1, 0.2
Cutting edge radius (mm)	0.03, 0.05
Length of cut (mm)	6
Tool's rake angle, α (°)	10
Workpiece's initial temperature (°C)	20

Table 2: Chemical composition for AISI H13 in percentage by weight

Elements	C	Cr	Mn	Mo	Ni	Si	V
Weight (%)	0.38	5.02	0.33	1.35	0.12	0.94	0.12

2.2. Design of experiment

The simulation was done using four factors at two levels design of experiment of Taguchi method $L_8(2^7)$ orthogonal array [21]. This type of orthogonal array is chosen because it has the ability in checking iterations between factors where every row of the matrix represents one trial but in randomized orders. The two levels of every factors were represented in the matrix by numerals of '0' and '1' or '1' and '2'. Factors and levels which was used throughout the simulation was tabulated in Table 3 and the cutting parameter combination adopted in Taguchi method $L_8(2_7)$ orthogonal array was presented through Table 4.

Table 3: Levels and factors applied in AdvantEdge finite element simulation (radial width of cut is kept constant at 6 mm)

Factors	Level	
	1	2
A - cutting speed, v_c (m/min)	200	240
B - feed-rate, f_z (mm/tooth)	0.03	0.06
C - axial depth of cut, a_p (mm)	0.1	0.2
D - cutting-edge radius, r_n (mm)	0.03	0.05

Table 4: Cutting parameter combination adopted in Taguchi method $L_8(2_7)$ orthogonal array

Test no.	Cutting speed v_c (m/min)	Feed rate f_z (mm/tooth)	Axial depth of cut a_p (mm)	Cutting-edge radius r_n (mm)
1	200	0.03	0.1	0.03
2	200	0.03	0.2	0.05
3	200	0.06	0.1	0.05
4	200	0.06	0.2	0.03
5	240	0.03	0.1	0.05
6	240	0.03	0.2	0.03
7	240	0.06	0.1	0.03

8	240	0.06	0.2	0.05

3. Result and discussion

3.1. Cutting force

It is important to study the process involving cutting force such as temperature of the cutting, accuracy of the surface and worn of the tool because there are subjected to performance of the cutting force. Fig. 2a-h shows the outcome of the simulation regarding cutting force for variable machining parameters and rounded cutting-edge radius. From the figure, it can be understood that the results of feed-rate which are 0.03 and 0.06mm/tooth, respectively exhibit different emergent inclinations. For 0.03mm/tooth value of feed-rate, y-direction of cutting force is more sensitive than x-direction of cutting force where cutting force growths significantly to the highest value before drop drastically after length of cut is reached above 4.5 mm. This is attributable to the consequence of thermal softening and strain hardening of workpiece material since the cutting tool and the workpiece material have enough time to produce heat because of the longer contact time between them at lower feed rate than at high feed rate. On the other hand, cutting force for 0.06mm/tooth value of feed-rate presents an opposite trend where it quickly reached to the maximum value within 1.0 mm length of cut and constant cutting force is performed throughout the process attributable to strain hardening effect which is equivalent to thermal softening [22].

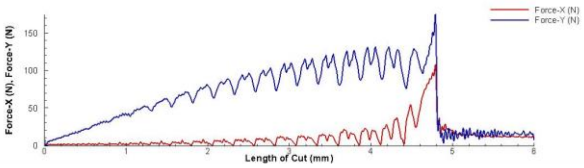

(a) Cutting force for test no. 1

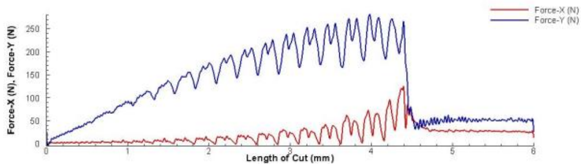

(b) Cutting force for test no. 2

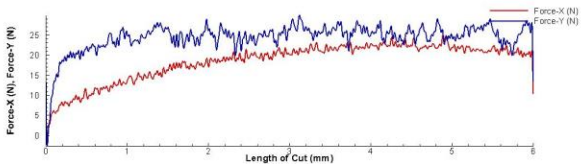

(c) Cutting force for test no. 3

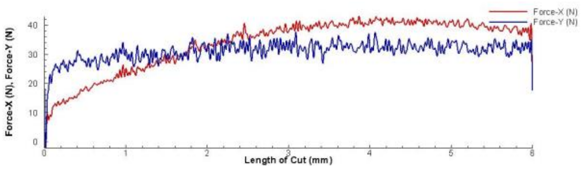

(d) Cutting force for test no. 4

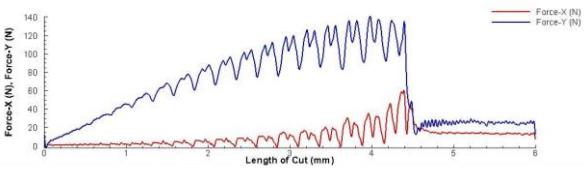

(e) Cutting force for test no. 5

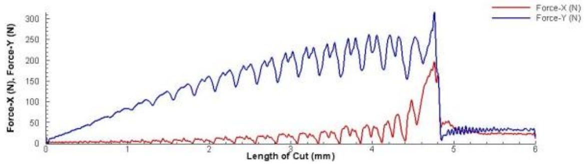

f) Cutting force for test no. 6

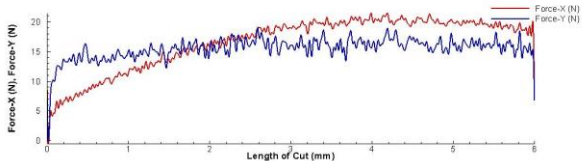

g) Cutting force for test no. 7

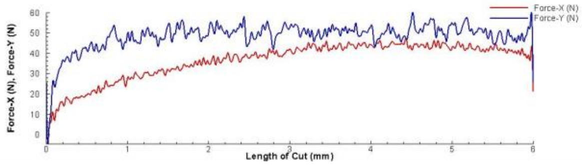

(h) Cutting force for test no. 8

Fig. 2a-h: Simulation result of cutting forces for variables machining parameters and rounded cutting-edge radius

Simulation results regarding the resultant of cutting force for variable machining parameters and rounded cutting-edge radius is tabulated in Table 5. The resultant of cutting force, F_r are calculated as shown in (1):

$$F_r = \sqrt{(F_x^2 + F_y^2)}$$

which F_x and F_y represent data points in the direction of X and Y of cutting forces, respectively.

Table 5: Resultant cutting force for the simulation results of the variable machining parameters and rounded cutting-edge radius

Test no.	Cutting speed v_c (m/min)	Feed-rate f_z (mm/tooth)	Axial depth of cut a_p (mm)	Cutting edge radius r_n (mm)	Resultant cutting force F_r (N)
1	200	0.03	0.1	0.03	197.23
2	200	0.03	0.2	0.05	308.70
3	200	0.06	0.1	0.05	37.64
4	200	0.06	0.2	0.03	56.64
5	240	0.03	0.1	0.05	152.00
6	240	0.03	0.2	0.03	368.92
7	240	0.06	0.1	0.03	28.32
8	240	0.06	0.2	0.05	75.60

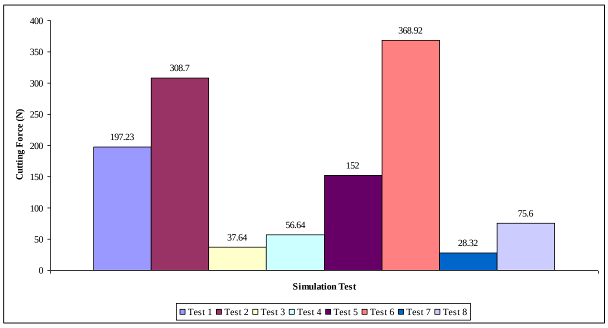

Fig. 3: Cutting force simulation results

Resultant of cutting force is observed to has the maximum value of 368.92 N when speed of the cutting is setting at 240 m/min, feed-rate at 0.03mm/tooth, depth of cut in axial direction at 0.2mm and cutting-edge at 0.03mm in radius. Increasing the value of depth of cut in axial direction also cutting-edge radius resulted in an increasing of resultant cutting force while constant speed of the cutting and feed-rate is taken place as shown in the result of simulation test no. 1 and 2 and the result of simulation test no. 7 and 8. Deeper depth of cut in axial direction showing that more material is being detached from the workpiece. Hence, resultant of cutting force is discovered to be increased as more energy is required due to the larger contact area between the cutting tool and workpiece material was increases as the deeper depth of cut was perform. Smaller radius of rounded cutting edge generates lower cutting forces than larger radius of rounded cutting edge. This was due to the tool easier enters the workpiece material as well less area of contact among cutting-edge and work surface thereby less friction is generated during the cutting process [8,23]. Rising the value of speed of the cutting and depth of cut in axial direction between simulation test no. 1 and simulation test no. 6 resulted in an increase of resultant cutting force by 46.54%. The results obtained is in parallel with the results published by the previous researchers [15,16]. This is because of the effect of strain hardening which is larger than the effect of thermal softening occurs during the cutting process at higher cutting speed. In contrast, rising the value of speed of the cutting and feed-rate as shown by simulation test no. 1 and no. 7 resulted in decreasing the resultant cutting force by almost 85.64% which may help to improve surface integrity of the machined workpiece material.

3.2. Cutting temperature

Temperature gives huge effect on life of cutting tool because materials will become weaker and softer as they become hotter which reducing the wear resistance of the cutting tool itself. Fig. 3 and Fig. 4 respectively shows the temperature distribution and maximum temperature region for the simulation model using 240m/min speed of cutting, 0.06mm/tooth of feed-rate, 0.1mm of cutting depth in axial direction and 0.03mm radius of cutting-edge. Table 6 and Fig. 5 tabulated and shows results for simulation of cutting temperature for variable machining parameters and rounded shape of cutting-edge radius. The maximum cutting temperature was indicated as 674.91°C at 240m/min speed of cutting, 0.06mm/tooth of feed-rate, 0.1mm of cutting depth in axial direction and 0.03mm radius of cutting-edge. The maximum cutting temperature obtained is lesser than the AISI H13 austenitizing temperature, therefore a layer known as white layer is supposedly hard to be created under the machining parameters and cutting geometry used in this study.

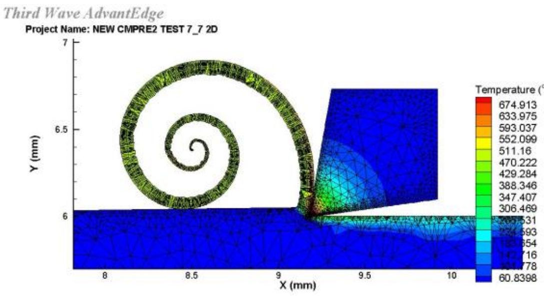

Fig. 4: Temperature distribution of the simulation model (v_c=240m/min, f_z=0.06mm/tooth, a_p=0.1mm, r_n=0.03 mm)

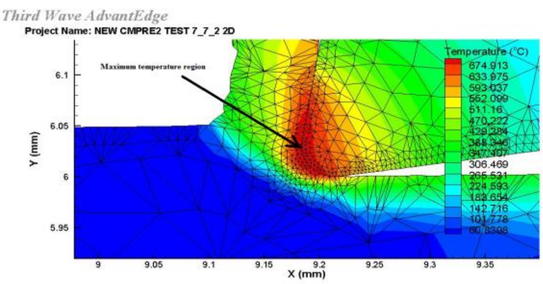

Fig. 5: Maximum temperature region of the simulation model (v_c=240m/min, f_z=0.06mm/tooth, a_p=0.1mm, r_n=0.03 mm)

The results of simulation test no. 1 and 7 and the simulation test no. 2 and 8 shows that increasing the cutting speed and the feed rate resulted in temperature rising from 598.16 °C to 674.91 °C and 626.59 °C to 650.70 °C which increment of almost 11.37 % and 3.71 %, respectively in terms of percentage value. The result of temperature rising may induce crater and flank wears in the cutting tool. Low speed of the cutting and feed-rate values induced low temperature for the cutting associated to the high speed of the cutting and feed-rate values. This is due to the heat diffusion which dissipated more heat as the longer contact time between cutting tool and workpiece material attaching together [7].

Table 6: Cutting temperature for the simulation results of the variable machining parameters and rounded cutting-edge radius

Test no.	Cutting speed v_c (m/min)	Feed-rate f_z (mm/tooth)	Axial depth of cut a_p (mm)	Cutting edge radius r_n (mm)	Cutting Temperature (°C)
1	200	0.03	0.1	0.03	598.16
2	200	0.03	0.2	0.05	626.59
3	200	0.06	0.1	0.05	662.94
4	200	0.06	0.2	0.03	644.67
5	240	0.03	0.1	0.05	634.00
6	240	0.03	0.2	0.03	602.00
7	240	0.06	0.1	0.03	674.91
8	240	0.06	0.2	0.05	650.70

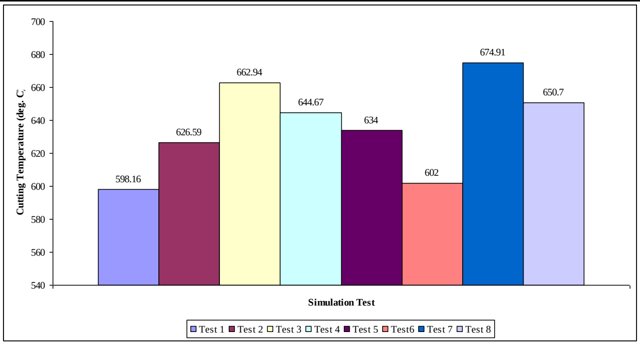

Fig. 6: Cutting temperature simulation results

Increasing cutting depth in axial direction and radius of cutting-edge resulted in an increase of cutting temperature as speed of the cutting and feed-rate is kept constant at low value of 200m/min and 0.03mm/tooth, respectively as shown on the simulation result test no. 1 and 2. Rising in cutting temperature of 4.5 % is related to more area of contact involving cutting-edge and work surface, thereby creating higher friction [24]. Meanwhile, at high value speed of the cutting and feed-rate which 240m/min and 0.06mm/tooth, correspondingly, the results of simulation test no. 7 and 8 shows the reduction of cutting temperature from 674.91 °C to 650.70 °C, which is 3.72 % in reduction although the cutting depth in axial direction and radius of the cutting-edge increases. The decreasing of cutting temperature at higher feed-rate and speed of the cutting is related to higher thermal softening than strain hardening occurs in workpiece material.

3.3. Chips morphology

The formation of all types of chips involves a shearing of the work material in the region of a plane extending, commencing the edge of tool towards the point of upper surface of chips leaves the surface of the workpiece material [25]. Fig. 7a-h and Table 7 shows and tabulated the simulation result of chips formation for variables machining parameters and rounded cutting-edge radius, respectively. The shape of the chips obtained can be categorized into two which are continuous chips and serrated chips. The difference between these two chips are depending on the value of feed-rate which 0.03mm/tooth of feed-rate tends to produce chips in serrated form while continuous chips are related to 0.06 mm/tooth of feed rate. This is in accordance to Vyas et al. [26] which stated that undeformed chip thickness in milling, which is the value of feed, is one of the conditions that control chip formation. Contact time between cutting tool and workpiece at lower feed rate is longer than at high feed rate, thus more heat is produced at cutting tool and workpiece, thus decreases the shear fracture strain of the material, thereby producing serrated chip.

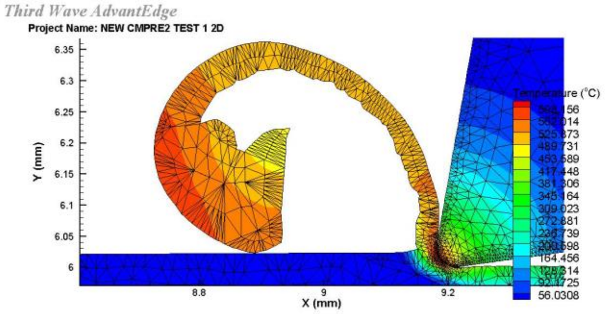

(a) Chip formation for test no. 1, r = 0.47

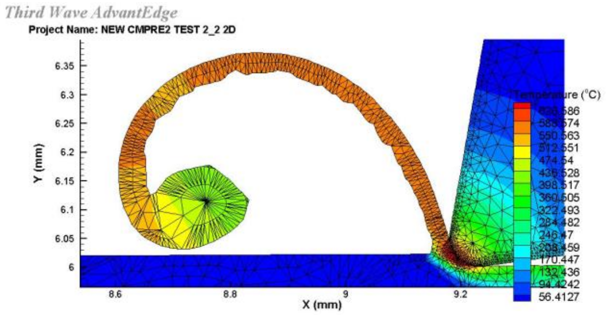

(b) Chip formation for test no. 2, r = 0.72

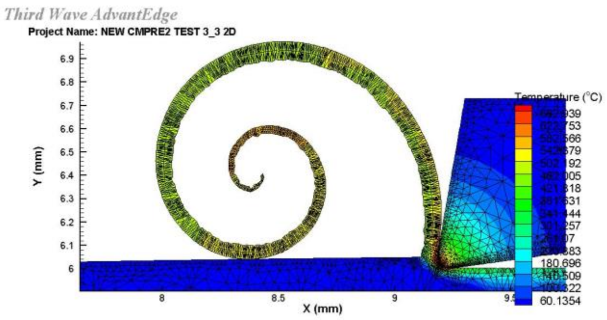

(c) Chip formation for test no. 3, r = 0.95

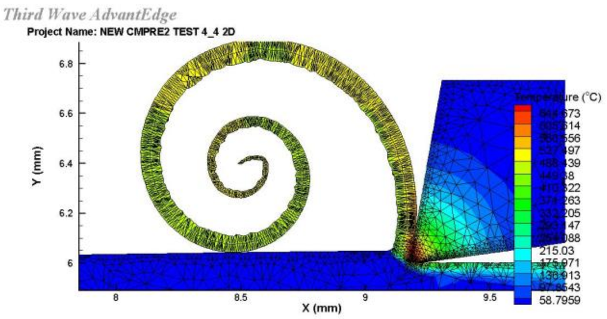

(d) Chip formation for test no. 4, r =0.99

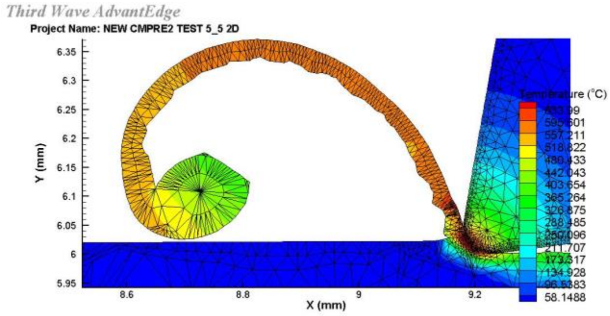

(e) Chip formation for test no. 5, r = 0.59

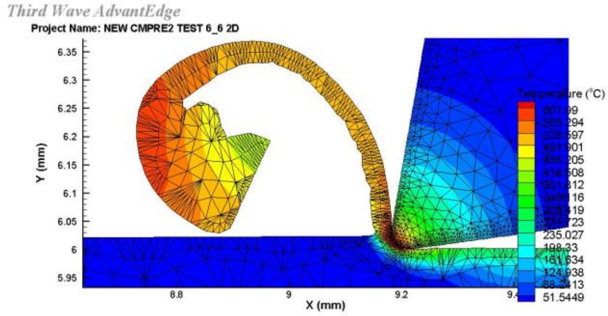

(f) Chip formation for test no. 6, r = 0.57

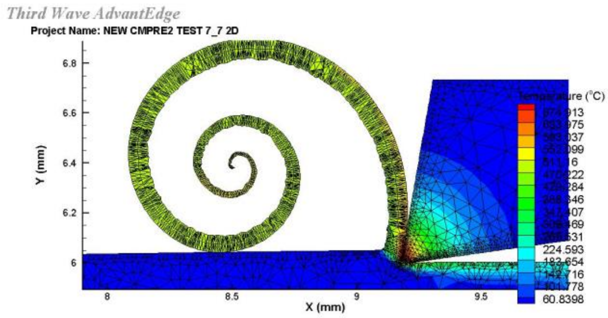

(g) Chip formation for test no. 7, r = 0.91

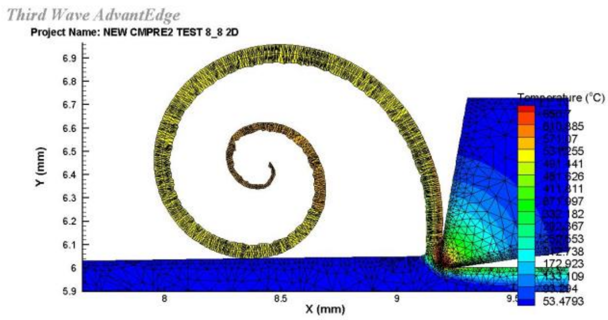

(h) Chip formation for test no. 8, r = 0.98

Fig. 7a-h: Simulation result of chip formation for variables machining parameters and rounded cutting-edge radius

Ratio of the chip thickness is calculated based on the Eq. (2):

Ratio of the chip thickness, $r = t_o / t_c$

which t_o represents the thickness of the chips preceding to formation of chips (feed) while t_c is the thickness of the chips after splitting from the workpiece materials. Thickness of the chips before doing the cutting process is always lesser than after, thereby value of ratio for chip thickness cannot be more than 1. The value of chip thickness ratio, r which tend to 1 is considered to be in continuous chips form while the value of chip thickness ratio, r which tends to 0 is considered to be in serrated chips form [25].

Table 7: Chip thickness ratio for the simulation results of the variable machining parameters and rounded cutting-edge radius

Test no.	Cutting speed v (m/min)	Feed rate f_z (mm/tooth)	Axial depth of cut a_p (mm)	Cutting edge radius r_n (mm)	Chip thickness ratio
1	200	0.03	0.1	0.03	0.47
2	200	0.03	0.2	0.05	0.72
3	200	0.06	0.1	0.05	0.95
4	200	0.06	0.2	0.03	0.99
5	240	0.03	0.1	0.05	0.59
6	240	0.03	0.2	0.03	0.57
7	240	0.06	0.1	0.03	0.91
8	240	0.06	0.2	0.05	0.98

The value of ratio for chip thickness obtained is parallel in shape with the chips formed. Highest value of ratio is observed at 0.06mm/tooth of feed-rate with the ratio value of 0.99 and chips in continuous form are produced. In contrast, the smallest value of ratio for chip thickness is observed at 0.03mm/tooth of feed-rate which the ratio value is 0.47 and chips with serrated form is produced.

4. Conclusions

From the simulation results obtained, conclusions can be made which increasing value of cutting depth in axial direction and rounded cutting-edge radius resulted in increasing the force and temperature of the cutting, respectively. Furthermore, increasing value of speed of the cutting as well as feed-rate result in decreasing value of cutting force but increasing the value of cutting temperature. Smaller radius generates lower cutting forces than larger radius of rounded cutting edge thus may help to improve the surface integrity of the machined workpiece material. Chip formed is mostly related to the feed rate which smaller value of feed rate produce the serrated chip formed while larger value of feed rate producing continuous chip form. The highest temperature of the cutting is 674.91℃. The value obtained is lesser than the AISI H13 austenitizing temperature, therefore a layer known as white layer is supposedly hard to be created based on the cutting geometry and machining parameters applied. Due to that, rounded cutting edge radius of 0.03 mm and the cutting conditions of 240m/min speed of cutting, 0.06mm/tooth of feed rate and 0.1mm depth of cut in axial direction is recommended to be applied to cut workpiece material of AISI H13 (52HRC).

5. Acknowledgements

The authors would like to express gratitude to the Malaysian Government, Universiti Kebangsaan Malaysia for financial provision under grant number FGRS/1/2016/TK03/UKM/01/1 and HPMT Industries Sdn. Bhd.

References

[1] Wyen CF & Wegner K, "Influence of cutting edge radius on cutting forces in machining titanium", *CIRP Annals-Manufacturing Technology,* Vol.59, No.1, (2010), pp.93-96
[2] Denkena B, Kohler J & Ventura CEH, "Customized cutting edge preparation by means of grinding", *Precision Engineering* Vol.37, No.3, (2013), pp.590-598
[3] Yen YC, Jain A & Altan T, "A finite element analysis of orthogonal machining using different tool edge geometries", *Journal of Material Processing Technology* Vol.146, No.1, (2004), pp.72-81
[4] Rech J, "Influence of cutting edge preparation and surface issues", *International Conference Smart Solutions for Metal Cutting, HSS Forum Aachen*, (2005), pp.1-12
[5] Bassett E, Kohler J & Denkena B, "On the honed cutting edge and its side effect during orthogonal turning operation of AISI1045 with coated WC-Co inserts", *CIRP Journal of Manufacturing Science and Technology*, Vol.5, No.2, (2012), pp.108-126
[6] Kandrac L, Mankova I & Vrabel M, "Cutting edge preparation in machining process", *Zeszyty Naukowe Politechniki Rzeszowskiej, Mechanics*, Vol.85, No.2, (2013), pp.149-159
[7] Wang CY, Tian JJ, An QL & Chen M, "Numerical investigation on effect of rounded cutting edge radius in milling of ultra-high-strength steel 30Cr3SiNiMoVA", *Advanced Materials Research,* Vol.797, (2013), pp.202-207
[8] Afazov S, Ratchev S & Segal J, "Effect of the cutting tool edge radius on the stability lobes in micro milling", *Advanced Materials Research,* Vol.223, (2011), pp.859-868
[9] M'Saoubi R & Chandrasekaran H, "Investigation of the effect of tool micro-geometry and coating on tool temperature during orthogonal turning of quenched and tempered steel", *International Journal of Machine Tools and Manufacture*, Vol.44, No.2-3, (2004), pp.213-224
[10] Quteiro JC, Dias AM & Jawahir IS, "On the effects of residual stresses induced by coated and uncoated cutting tools with finite edge radii in turning operations", *CIRP Annals,* Vol.55, No.1, (2006), pp.111-116
[11] Zhang Q, Zhang S & Li J, "Three dimensional finite element simulation of cutting forces and cutting temperature in hard milling of AISI H13 steel", *Procedia Manufacturing*, Vol.10, (2017), pp.37-47
[12] Riza M & Adesta EYT, "Investigation of cutting temperature for AISI H13 in high speed end milling", *International Journal of Engineering Materials and Manufacture,* Vol. 1, No.1, (2016), pp.27-34
[13] Sato M, Tamura N & Tanaka H, " Temperature variation in the cutting tool in end milling", *Journal of Manufacturing Science and Engineering*, Vol.133, No.2, (2011), pp.1-7
[14] Coz GL & Dudzinski D, "Temperature variation in the workpiece and in the cutting tool when dry milling Inconel 718", *The International Journal of Advanced Manufacturing Technology,* Vol.74, No.5-8, (2014), pp.1133-1139
[15] Wang F, Tao Q, Xiao L, Hu J & Xu L, "Simulation and analysis of serrated chip formation in cutting process of hardened steel considering ploughing-effect", *Journal of Mechanical Science and Technology,* Vol.32, No.5, (2018), pp.2029-2037
[16] Cui X, Zhao J & Tian X, "Cutting forces, chip formation, and tool wear in high-speed face milling of AISI H13 steel with CBN tools", *The International Journal Advance Manufacturing Technology,* Vol.64, No. 9-12, (2013), pp.1737-1749
[17] Outeiro J, "Optimization of machining parameters for improved surface integrity of AISI H13 tool steel", *Machines et Usinage a Grande Vitesse (MUGV) France,* (2012), pp.1-10
[18] Li B, Zhang S, Yan Z & Zhang J, "Effect of edge hone radius on chip formation and its microstructural characterization in hard milling of AISI H13 steel", *The International Journal of Advanced Manufacturing Technology,* (2018), pp.1-14
[19] Afazov SM, Ratchev SM & Segal J, "Prediction and experimental validation of micro-milling cutting forces of AISI H13 steel at hardness between 35 and 60 HRC", *The International Journal Advance Manufacturing Technology,* Vol.62, No.9-12, (2012), pp.887-899
[20] Zhang S & Guo YB, "An experimental and analytical analysis on chip morphology, phase transformation, oxidation, and their relationships in finish hard milling", *International Journal of Machine Tools and Manufacture,* Vol.49, No.11, (2009), pp.805-813
[21] Park SH, *Robust Design and Analysis for Quality Engineering,* Chapman & Hall, London, UK (1996), pp:68-69.
[22] Hou J, Zhou W, Duan H, Yang G, Xu H & Zhao N, "Influence of cutting speed on cutting force, flank temperature, and tool wear in end milling of Ti-6Al-4V alloy", *The International Journal Advance Manufacturing Technology*, Vol.70, No.9-12, (2014), pp.1835-1845
[23] Bogdan BM, Sabin PM, Stefan S & Dan P, "Unconventional technologies in preparation of microgeometry edges on cutting tools", *Romanian Association of Nonconventional Technologies,* (2013), pp.10-16
[24] Bouzakis KD, Michailidis N, Skordaris G, Kombogiannis S, Ha ijiyiannis S, Efstathiou K, Erkens G, Rambadt S & Wirth I, "Effect of the cutting edge radius and its manufacturing procedure, on the milling performance of PVD coated cemented carbide inserts", *CIRP Annals*, Vol.51, No.1, (2002) pp.61-64
[25] Trent EM & Wright PK, *Metal Cutting,* Butteworth-Heinemann, Woburn, MA, (2000), pp:23.
[26] Vyas A & Shaw MC, "Mechanics of saw-tooth chip formation in metal cutting", *Journal of Manufacturing Science & Engineering,* Vol.121, No.2, (2008), pp.163-172